Paratope Plasticity in Diverse Modes Facilitates Molecular Mimicry in Antibody Response

Lavanya Krishnan, Suvendu Lomash, Beena Patricia Jeevan Raj, Kanwal J. Kaur and Dinakar M. Salunke

J Immunol 2007;178;7923-7931

The Journal of Immunology is published twice each month by
The American Association of Immunologists, Inc.,
9650 Rockville Pike, Bethesda, MD 20814-3994.

Print ISSN: 0022-1767 Online ISSN: 1550-6606.

Paratope Plasticity in Diverse Modes Facilitates Molecular Mimicry in Antibody Response[1]

Lavanya Krishnan, Suvendu Lomash, Beena Patricia Jeevan Raj, Kanwal J. Kaur, and Dinakar M. Salunke[2]

The immune response against methyl-α-D-mannopyranoside mimicking 12-mer peptide (DVFYPYPYASGS) was analyzed at the molecular level towards understanding the equivalence of these otherwise disparate Ags. The Ab 7C4 recognized the immunizing peptide and its mimicking carbohydrate Ag with comparable affinities. Thermodynamic analyses of the binding interactions of both molecules suggested that the mAb 7C4 paratope lacks substantial conformational flexibility, an obvious possibility for facilitating binding to chemically dissimilar Ags. Favorable changes in entropy during binding indicated the importance of hydrophobic interactions in recognition of the mimicking carbohydrate Ag. Indeed, the topology of the Ag-combining site was dominated by a cluster of aromatic residues, contributed primarily by the specificity defining CDR H3. Epitope-mapping analysis demonstrated the critical role of three aromatic residues of the 12-mer in binding to the Ab. Our studies delineate a mechanism by which mimicry is manifested in the absence of either structural similarity of the epitopes or conformational flexibility in the paratope. An alternate mode of recognition of dissimilar yet mimicking Ags by the anti-peptide Ab involves plasticity associated with aromatic/hydrophobic and van der Waals interactions. Thus, antigenic mimicry may be a consequence of paratope-specific modulations rather than being dependent only on the properties of the epitope. Such modulations may have evolved toward minimizing the consequences of antigenic variation by invading pathogens. ***The Journal of Immunology,*** **2007, 178: 7923–7931.**

Molecular mimicry is the antithesis to the specificity of recognition processes as exemplified by the immune system. The hallmark of the acquired immune system is its ability to distinguish between distinct molecules. Specificity at the molecular level enables immune responses to be mounted against the invading pathogens while ensuring self-nonself discrimination. Molecular mimicry, in essence, is the breakdown of the specificity of recognition of humoral and cellular responses. The physiological equivalence of disparate molecular entities has substantive implications in immunological processes that confront the repertoire of antigenic diversity. Although molecular mimicry has been the central premise in the etiology and pathogenesis of self-reactive Abs and T cells (1, 2), it also provides an archetypal model for mechanistic understanding of the specificity and complexity of immune recognition. Exploration of diverse facets of molecular mimicry would provide insights into the genesis of autoimmunity and aid vaccine design strategies (3).

We have addressed the molecular basis of mimicry by analyzing chemically dissimilar ligands which show equivalence to an impressive degree (4–12). Con A, a mannose-specific lectin, has been shown to recognize Tyr-Pro-Tyr motif-containing peptides (13, 14). However, in the crystal structures of the complexes of a number of such peptides with the lectin, well-defined structural similarity could not be deciphered as the carbohydrate and peptide ligands did not bind at a common site (5, 6, 8, 9). Similarly, functional mimicry between the 12-mer (DVFYPYPYASGS) and methyl-α-D-mannopyranoside was demonstrated in polyclonal responses in terms of cross-reactivity wherein immunization with the peptide gave rise to carbohydrate-recognizing Abs and vice versa (4). In addition, during immune maturation, a booster with the peptide Ag could also enhance the anti-mannopyranoside Ab response, thus establishing equivalence between the peptide and carbohydrate moieties (7). However, precise molecular description of the functional mimicry, as seen by the immune system, between these otherwise chemically independent Ags remained elusive.

Previous investigations had suggested that the ability to recognize mimicking Ags arose from the conformational flexibility in the Ab paratope through adaptation of structure appropriate for complementing the Ag (12). The present study addresses the physicochemical basis of mimicry in humoral responses against a peptide and a carbohydrate at the monoclonal level. Molecular mimicry between 12-mer and mannopyranoside was analyzed in terms of recognition specificity and affinity of interaction with the mimicking Ags. Quantification of the changes that occur upon binding in terms of kinetic and thermodynamic parameters and the effect of temperature on these would shed light on the modes of binding of diverse yet mimicking Ags. Furthermore, a systematic understanding of the energetics of Ag binding and its correlation with the structural features of the combining site of the Ab would facilitate better understanding of the phenomenon of molecular mimicry in the humoral response. Our studies highlight the role of Ab paratope in the generation of diverse mimotope-recognition modes, revealing a new facet of the evolving paradigm in molecular mimicry. Modulation of mimicry by Ab-dependent properties suggests mechanisms by which the host can evolve strategies for minimizing the consequences of antigenic variation by the pathogen.

National Institute of Immunology, New Delhi, India

Received for publication January 31, 2007. Accepted for publication March 29, 2007.

The costs of publication of this article were defrayed in part by the payment of page charges. This article must therefore be hereby marked *advertisement* in accordance with 18 U.S.C. Section 1734 solely to indicate this fact.

[1] This work was supported by the Department of Biotechnology, Government of India. L.K. was a recipient of a fellowship from the Council of Scientific and Industrial Research (India).

[2] Address correspondence and reprint requests to Dr. Dinakar M. Salunke, National Institute of Immunology, Aruna Asaf Ali Road, New Delhi 100 067 India. E-mail address: dinakar@nii.res.in

Materials and Methods

Preparation of Ags and generation of hybridomas

The 12-mer (DVFYPYPYASGS) peptide was synthesized and conjugated to BSA and diphtheria toxoid (DT)[3] as reported previously (12). Mannopyranoside-BSA was prepared after activation of *p*-aminophenyl-α-D-mannopyranoside (Sigma-Aldrich) with an equimolar amount of glutaraldehyde in 0.1 M sodium carbonate buffer (pH 9.0), for 30 min at room temperature, and then mixing with BSA. The reaction mixture was incubated at 4°C overnight, after which it was extensively dialyzed against normal saline.

Previously standardized protocols for immunizations were followed wherein each mouse was injected i.p. with 200 μg of conjugated 12-mer-DT emulsified with CFA (Difco) and given a booster of the Ag with IFA (Difco) on day 21. The highest responder mouse was sacrificed for harvesting spleen cells that were allowed to fuse with the Sp2/O myeloma cells, growing in the log phase, using PEG1600 for the generation of hybridomas and subjected to hypoxanthine-aminopterin-thymidine selection in DMEM (Biological Industries). The culture supernatant of the hybrid cells was screened for the presence of 12-mer and mannopyranoside-recognizing Ab by ELISA. The positive clones were further subcloned using a limited dilution technique to ensure monoclonality.

Ab purification

The Ab was purified from the ascitic fluid of mice by an initial partial purification by salt fractionation with a 40% ammonium sulfate cut. The precipitated Ab was then solubilized and dialyzed in 10 mM Tris-Cl (pH 8.5), and subjected to anion exchange chromatography on a DEAE column. The purity of the Ab was checked by SDS-PAGE and concentration was estimated by protein assay (Bio-Rad) using BSA as the standard.

ELISAs

The binding of the Abs, from cell supernatant or in purified form, to the peptide and carbohydrate ligands was assayed by sandwich ELISA. 12-mer-BSA or mannopyranoside-BSA was used as the coating Ag at a concentration of 2 μg/well on 96-well immunosorbent plates and Ab was added at appropriate dilutions after blocking with 1% BSA. HRP-labeled goat anti-mouse IgG (Jackson ImmunoResearch Laboratories) was used as the secondary Ab and *o*-phenylenediamine (Sigma-Aldrich) and H_2O_2 as peroxidase substrates. Absorbance was recorded at 490 nm after addition of 1 N H_2SO_4. For Ab isotype determination, goat anti-mouse isotype alkaline phosphatase-labeled Ab (Santa Cruz Biotechnology) was used. The protocol for competitive ELISA included incubation of constant amounts of Ab with varying amounts of the mimicking Ags (in their BSA-conjugated form) and monitoring of the binding of the remaining free Ab to the immobilized mannopyranoside and 12-mer. The level of inhibition was calculated by comparison of binding signal of the Ab incubated with different ligand concentrations with respect to signal of Ab containing no soluble ligand and expressed as a percentage.

Measurement of binding kinetics

Biospecific-interaction analysis was performed using a BIAcore 2000 Biosensor System (Amersham Biosciences). Both 12-mer-BSA and mannopyranoside-BSA were immobilized onto CM4 (carboxymethylated)-certified grade sensor chips using an equal mixture of EDC/NHS (*N*-ethyl-*N*-(dimethylaminopropyl) carbodiimide; *N*-hydroxysuccinimide) in 10 mM sodium acetate buffer (pH 4.5). Approximately 500 resonance units (RU) of conjugate were immobilized in each case, where 1000 RU corresponds to an immobilization level of ~1 ng/mm^2. The unreacted activated sites were blocked with 1 M ethanolamine. The reference surface was treated in the same way except that no ligand was passed over this surface to normalize the chemistries between the two flow cells.

Binding studies were conducted in 10 mM HEPES (pH 7.4), containing 150 mM NaCl, 3.0 mM EDTA, and 0.005% surfactant P20 at 15°C, 20°C, 25°C, and 30°C. For the determination of association rate constant (k_a; $M^{-1}s^{-1}$), various concentrations of Ab in binding buffer were allowed to bind to the immobilized ligands at a flow rate of 30 μl/min. The dissociation rate constant (k_d; s^{-1}) was measured by replacing with binding buffer. Regeneration was conducted using 10 mM glycine-HCl (pH 2.2).

Analysis was done by BIAevaluation 3.2 software wherein the sensograms were fit globally using the simultaneous k_a/k_d menu which first generates the rate equations for the model used and then finds the values for the parameters in the rate equation that best fit the experimental data. The data were fit to the bivalent model of interaction and described using the first set of rate constants for both phases of binding that were used to derive the equilibrium dissociation constant ($K_D = k_d/k_a$). Although the calculated maximum response, R_{max} was in the range of 30–66 RU, the χ^2 and residuals of the fit of the experimental data to the model were 0.3–1.6 and ±2 to ±5, respectively.

Thermodynamic analysis of Ag binding

A binding interaction is defined by a net negative change in the Gibbs free energy at equilibrium (ΔG_{eq}) such that $\Delta G_{eq} = RT \ln K_D$, where R is the Rydberg's gas constant, and T is the temperature in Kelvin.

The energetics during the association or dissociation phase result from changes in enthalpy (ΔH) and entropy (ΔS). Although the enthalpy term generally describes heat changes that take place due to interactions at the binding interface, entropy changes largely represent net conformational perturbations that occur either within the interacting entities or in the solvent molecules and are considered to reflect the role of hydrophobic interactions during complexation. Thus, the free energy changes that accompany either an association or dissociation step are defined by $\Delta G_{a/d} = \Delta H_{a/d} - T\Delta S_{a/d}$, such that $\Delta G_{eq} = \Delta G_a - \Delta G_d$.

The changes in enthalpy and entropy associated with the two phases in binding as well as the corresponding net values at equilibrium can be obtained from the activation energy (*Ea*) that can be calculated from the slopes of the Arrhenius plots considering the changes in heat capacity as a function of temperature to be zero. The individual thermodynamic parameters for both the association and the dissociation steps were calculated using the equations: $\Delta H_{a/d} = Ea - RT$ and $\ln (k_{a/d}/T) = -\Delta H_{a/d}/RT + T\Delta S_{a/d}/R + \ln(K'/h)$.

In these equations, T represents temperature in Kelvin, R the Rydberg gas constant, K' the Boltzmann's constant, and h the Planck's constant.

Ab sequencing

Approximately 10^6 to 10^7 hybridoma cells were used for total RNA extraction with TRIzol reagent (Invitrogen Life Technologies). Protocols followed for synthesis of the first strand of cDNA were identical with that reported earlier (12) except that a λ chain 3′ primer (Mouse Ig-Primer set; Novagen) was used in the case of L chain of mAb 7C4 and for H chain, 5′-GGCCAGTGGATAGAC-3′ primer was used as the 3′ primer. Subsequent amplification of the single-stranded cDNA by PCR was conducted using the 5′ and 3′ primers (Mouse Ig-Primer set; Novagen) for the L chain and 5′-AGGT(C/G)(A/C)A(A/G)CTGCAG(G/C)AGTC(A/T)GG-3′ as the 5′ primer and 5′-GGCCAGTGGATAGAC(T/C/A)GA-3′ as the 3′ primer for the H chain. A total of 3 μl of the PCR product was analyzed on 1% agarose gel. Subsequently, the PCR products were sequenced using their respective forward and reverse primers.

Molecular modeling

Homology modeling of proteins depends on the identification of a protein of known structure that shares sequence, properties, function, and/or evolutionary classification with the protein of interest. The search for structures with sequence similarities to our Ab was performed using the basic local alignment search tool (15) in the Protein Data Bank (PDB). As we were primarily studying the Ag-binding site, only the V regions of the Ab have been modeled. To optimize the juxtaposition of the V_L and V_H, we selected the template for modeling based on highest homology with both chains of the Ab rather than selecting two different Abs that show higher identity, individually, with each of the chains.

The structure of the Fab of an anti-hapten catalytic Ab 34E4 (PDB ID: 1Y0L) that catalyzes the conversion of benzisoxazoles to salicylonitriles was used as the template for homology based modeling of the mAb 7C4 Fv. Sequence alignment with 1Y0L showed a two-residue gap in CDR H3. Loop searches in the PDB database were conducted for the entire CDR tethering 3 residues on either side. Each of the top 10 options was individually screened for steric clashes with the neighboring residues. The loop conformation that did not show any steric clashes was selected.

The AMBER force field was used for energy-dependent analyses. Subsequent to homology modeling of mAb 7C4 Fv, the structure was energy minimized in the DISCOVER module of INSIGHT II (Accelerys) with 100 steps of steepest descent minimization followed by 400 steps of conjugate gradient minimization with gradually decreasing tethering of the backbone of the structure. The resultant structure was subsequently validated in terms of its stereochemistry using PROCHECK (16).

Synthesis and assay of the peptide analogs on solid surface

Sequentially mutating each residue of the 12-mer peptide to glycine and measuring the binding of the individual peptide analogs to the Ab would allow delineation of the Ab-specific epitope of the 12-mer. The 12-mer peptide analogs were synthesized on the surface of polyethylene pins

[3] Abbreviations used in this paper: DT, diphtheria toxoid; RU, resonance unit.

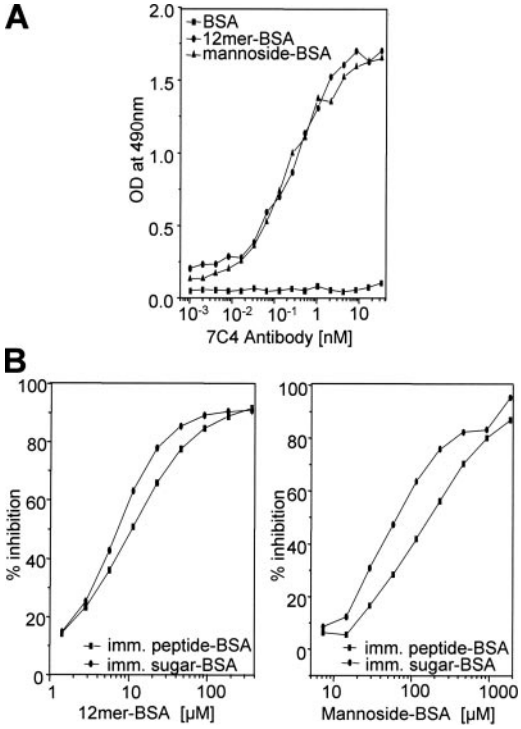

FIGURE 1. Comparative reactivity of the immunizing 12-mer and its mimicking mannopyranoside to the anti-peptide mAb 7C4. *A*, Binding of the Ab to the immobilized Ags, as analyzed by ELISA. A total of 2 μg/well mannopyranoside and 12-mer conjugated to BSA was used as coating Ags for ELISA. *B*, Competitive inhibition profile for binding to immobilized Ags by 12-mer-BSA and mannopyranoside-BSA in solution. The plot shows percentage inhibition in binding to the immobilized peptide and sugar Ags by the Ab in the presence of various concentrations of competing BSA-conjugated ligands, as detected by ELISA.

using F-moc chemistry as described previously (12). After completion of the synthesis, all peptide analogs were acetylated at the N terminus and side chains were deprotected. The pins with their irreversibly bound peptide analogues could be reused by removing the bound Ab by sonication in the recommended disruption buffer. Evaluation of Ab binding to the analogs was carried using an ELISA-based assay wherein 2% gelatin in PBS containing 0.1% Tween 20, for 2 h at 37°C, was used to reduce nonspecific binding. Subsequently, the pins were incubated with an appropriate concentration of Ab in PBS overnight at 4°C. HRP-labeled goat anti-mouse Ab was used for detection along with the substrates, *o*-phenylenediamine (Sigma-Aldrich) and H_2O_2, and OD was measured after addition of 1 N H_2SO_4 at 490 nm.

To assess the relative contribution of various residues of the 12-mer in binding to the Ab, the change in the signal of binding to each peptide analog with reference to the native peptide was calculated. This change was expressed as percentage loss of the Ab binding with respect of the native peptide and was defined as: percentage of loss in Ab binding = $((B_{native} - B_{analog})/B_{native}) \times 100$, where B_{native} was the binding signal of the native peptide and B_{analog} was that of the analog as measured by ELISA. The percentage loss in Ab binding was then plotted against each glycine-substituted residue of the 12-mer peptide.

Results

Generation of the mimicry-recognizing mAb and its Ag-binding kinetics

Anti-12-mer IgG-secreting clones were selected from among a panel of hybridomas generated against the 12-mer conjugated to DT. All the clones which were specific to the immunizing peptide also recognized mannopyranoside and the highest affinity mAb, 7C4 (IgG1 isotype), was further investigated in the context of peptide-carbohydrate mimicry. The Ab was purified from ascites by 40% ammonium sulfate precipitation before ion exchange chromatography.

The purified Ab 7C4 showed equivalent binding to the immunizing 12-mer and its mannopyranoside mimic (Fig. 1*A*). It was therefore pertinent to analyze whether these mimicking Ags could displace each other during binding to the Ab. Owing to the size and nature of the Ags, BSA-conjugated forms of 12-mer and mannopyranoside were made to compete with their immobilized forms for binding to mAb 7C4 (Fig. 1*B*). It was found that both the peptide and the carbohydrate Ag can compete with one another suggesting that the Ab is capable of recognizing the mimicking ligands equivalently and with comparable affinities.

Toward understanding the mechanistic details of the Ab binding to the Ags, the kinetics of the interactions with the immunogen and its mimic were measured. Measurement of the affinity of mAb 7C4 for the 12-mer and mannopyranoside was conducted on the surface plasmon resonance-based biosensor, Biacore2000, at ambient temperature (25°C). Various kinetic parameters including association (k_a) and dissociation (k_d) rate constants of binding of the Ab with the two Ags were calculated (Table I).

Real-time binding measurements show that mAb 7C4 has similar affinities for 12-mer and mannopyranoside with an equilibrium dissociation constant (K_D) of 94.5 and 135.8 nM, respectively. The k_a and k_d for binding to both the ligands are also comparable. The kinetic parameters quantitatively reinforce the observation that mAb 7C4 not only binds to the immunizing 12-mer but also shows cross-reactivity to mannopyranoside with equivalent affinity. The modes of binding of the two Ags appear to be similar as the association and dissociation rate constants are comparable at ambient temperature.

Influence of temperature on kinetics of Ag-Ab interaction

Measurement of k_a and k_d, as a function of temperature, enables evaluation of the thermodynamics and energetics of binding of the Ab to these chemically dissimilar yet mimicking Ags. Correlation of these physical parameters with structural features of the paratope would help to delineate the modes and mechanisms of interaction of Ab with 12-mer and mannopyranoside. Sensograms were generated for the binding of the Ab to the two Ags and the data

Table I. *Kinetic parameters of the binding of mAb 7C4 to the peptide and carbohydrate Ags at different temperatures*

	DVFYPYPYASGS				Mannopyranoside			
Temp (°C)	$k_a \times 10^{-4}$ ($M^{-1}s^{-1}$)	$k_d \times 10^3$ (s^{-1})	K_D (nM)	$t_{1/2}$ (s)	$k_a \times 10^{-4}$ ($M^{-1}s^{-1}$)	$k_d \times 10^3$ (s^{-1})	K_D (nM)	$t_{1/2}$ (s)
15	6.02 ± 0.07	1.30 ± 0.02	21.3	533.1	3.37 ± 0.04	3.03 ± 0.06	89.9	228.7
20	5.98 ± 0.11	3.84 ± 0.09	64.2	180.4	3.91 ± 0.02	3.93 ± 0.02	100.5	176.3
25	5.84 ± 0.11	5.52 ± 0.12	94.5	125.5	3.29 ± 0.08	4.47 ± 0.17	135.8	155.0
30	5.43 ± 0.08	6.86 ± 0.11	126.3	101.0	2.98 ± 0.10	4.80 ± 0.21	161.1	144.4

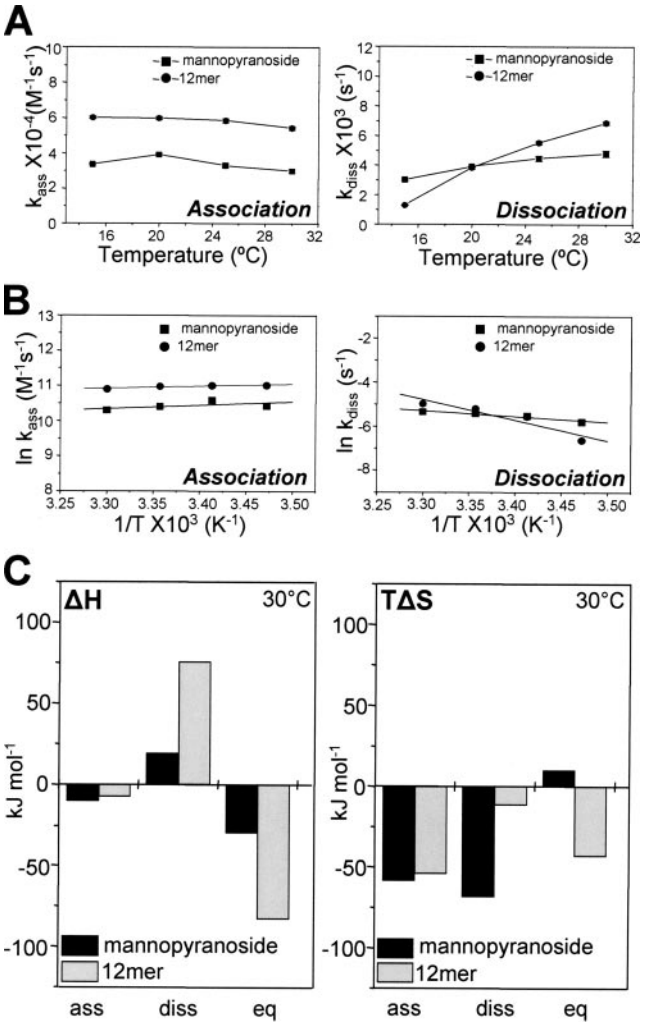

FIGURE 2. Thermodynamics of the binding of mAb 7C4 to the peptide immunogen and its mimicking carbohydrate Ag. *A*, Variation in the association (k_a) and dissociation (k_d) rate constants of the binding of mAb 7C4 to 12-mer and mannopyranoside with temperature. *B*, Arrhenius plots for the calculation of activation energy (*E*a) during each phase wherein the natural log of k_a or k_d has been plotted against the inverse of temperature. *C*, The comparison of the changes in enthalpy (ΔH) and entropy ($T\Delta S$) of binding to mannopyranoside and 12-mer peptide by mAb 7C4 at 30°C.

were analyzed using BIAevaluation 3.2 to determine the values of the association and dissociation rate constants of binding at different temperatures (Table I).

The affinity of the Ab 7C4 for both 12-mer and mannopyranoside does not undergo any significant change on increasing the temperature from 15 to 30°C (Table I). The kinetics of binding to both the peptide and carbohydrate as a function of temperature appear to be similar during the association phase (Fig. 2*A*). In contrast, during the dissociation phase, while kinetics of mannopyranoside binding were insensitive to changes in temperature, there was a marginal increase in k_d of mAb 7C4 binding to 12-mer (Fig. 2*A*). This is also reflected in the strength of the Ab-Ag complex, the half-life of which decreases by ~2- and 5-fold while binding to mannopyranoside and 12-mer, respectively (Table I).

Thus, the binding of the anti-peptide mAb 7C4 to the immunogen and its mimicking Ag does not appear to be significantly influenced by variation in temperature. The decrease in the affinity at higher temperature is similar to that observed for other protein-ligand interactions that do not undergo major conformational changes during binding (17, 18, 12).

Table II. *Changes in Gibbs free energy (ΔG) at equilibrium as a function of temperature during binding of mAb 7C4 to 12-mer and mannopyranoside*

Temp (°C)	ΔG_{eq} (kJ mol^{-1}) DVFYPYPYASGS	Mannopyranoside
15	−42.8	−38.8
20	−40.3	−39.2
25	−40.1	−39.2
30	−40.0	−39.6

Energetics of Ag binding

To gain insights into the possible modes of binding, the energetics of interactions of 12-mer and mannopyranoside were analyzed in the context of the nature of the mAb 7C4-binding site. The change in Gibbs free energy (ΔG_{eq}), a measure of the favorability of a reaction, can be calculated from the K_D such that the variation in the affinity of the Ab for the Ags can be directly correlated to the thermodynamics of binding to them. The change in ΔG_{eq} of mAb 7C4 binding to 12-mer and mannopyranoside, as a function of temperature, was ~−2 kJ/mol (Table II). Thus, consistent with the lack of variation in the affinity (K_D), there do not appear to be any significant temperature-dependent changes in the free energy of binding of the Ab to either of the mimics.

The effect of temperature variation on Ag binding was further analyzed by computing changes in enthalpy (ΔH) and entropy ($T\Delta S$) for the association and dissociation phases as well as at equilibrium. The activation energy (*E*a) for either phase of binding was determined from the slope of Arrhenius plot which enabled calculation of changes in ΔH and $T\Delta S$ at 30°C (Fig. 2*B*). It is interesting to note that while binding to the 12-mer is driven by favorable changes in enthalpy alone that to mannopyranoside is propelled by favorable changes in both enthalpy and entropy (Fig. 2*C*). The large negative, and therefore favorable, change in enthalpy (ΔH_{eq} is −83 kJ/mol) more than compensates for the unfavorable entropy change ($T\Delta S_{eq}$ equals −43 kJ/mol) and drives the 12-mer binding. In contrast, binding of mAb 7C4 to the mimicking carbohydrate is characterized by favorable changes in both ΔH_{eq} (−30 kJ/mol) and $T\Delta S_{eq}$ (10 kJ/mol).

Comparable changes in enthalpy and entropy occur during the association phase of binding to either Ag. The favorable change in ΔH_a of mAb 7C4 binding to the 12-mer is reinforced by unfavorable ΔH_d. This results in large negative enthalpy at equilibrium that overrides the unfavorable $T\Delta S_{eq}$, thus driving the binding to the peptide immunogen (Fig. 2*C*). During binding to mannopyranoside, the net negative ΔH_{eq} is contributed by both favorable changes in ΔH_a and unfavorable changes in ΔH_d (Fig. 2*C*). Additionally, large unfavorable $T\Delta S_d$ results in positive and thus favorable net change in entropy. Consequently, the net negative ΔG_{eq} at 30°C, during Ab-mannopyranoside complexation, is contributed by favorable changes in $T\Delta S_{eq}$ and ΔH_{eq}. Thus, binding of the mimicry recognizing Ab 7C4 to the sugar and peptide Ags differs mainly in the relative contributions of changes in enthalpy and entropy during the dissociation phase; while dissociation of mannopyranoside is disallowed by a negative $T\Delta S_d$, unfavorable ΔH_d does not favor the dissociation of 12-mer. Favorable changes in entropy that accompany the binding of the carbohydrate ligand may indicate the critical role of hydrophobic interactions in complex formation (19).

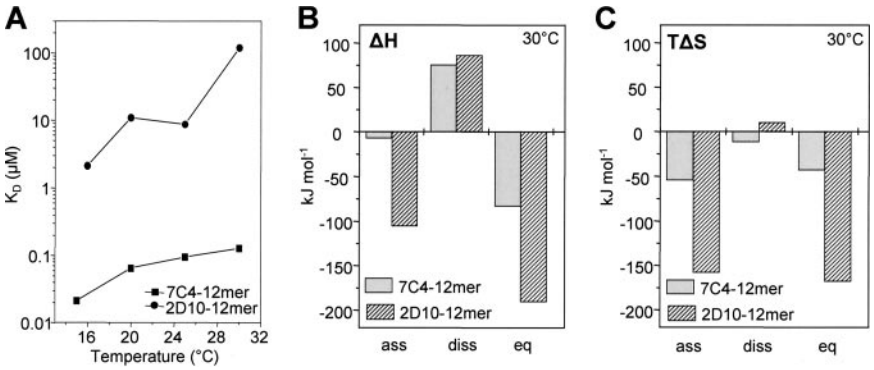

FIGURE 3. Comparison of thermodynamics of binding to 12-mer by mimicry-recognizing anti-peptide and anti-carbohydrate Abs. *A*, Effect of temperature on the kinetics of interaction between the 12-mer and mAb 7C4 and mAb 2D10. Changes in (*B*) enthalpy (ΔH) and (*C*) entropy ($T\Delta S$) during binding of the two Abs to 12-mer peptide at 30°C.

Ag binding by the anti-peptide and anti-carbohydrate Abs

To compare and contrast the modes of recognition by the anti-peptide and anti-carbohydrate Abs, both of which recognize the mimicry between mannopyranoside and 12-mer, analyses of the kinetics of peptide binding by the previously generated anti-mannopyranoside mAb, 2D10 (12), were also conducted. Unlike the binding of mAb 7C4, that of mAb 2D10 to the 12-mer was drastically influenced by changes in temperature; while k_a decreased by >8-fold, k_d of mAb 2D10 binding to 12-mer increased 6-fold. This results in >50-fold loss in 12-mer affinity to mAb 2D10 at 30°C as compared with a 5-fold loss in the case of Ab 7C4-12-mer interaction (Fig. 3*A*). Consequently, the free energy of the interaction of the Ab 2D10 with 12-mer is less favorable by about −10 kJ/mol at 30°C, while the stability of the mAb 7C4-12-mer complex appears to be comparatively insensitive to temperature. Drastic variation in the kinetics of binding as a function of temperature suggests that large structural changes may occur during mAb 2D10-12-mer complexation. Comparatively, the mAb 7C4-binding site may not undergo major conformational alteration during binding of either ligand and structural variability in its paratope may be limited.

Comparison of the energetics of binding to 12-mer by the anti-peptide mAb 7C4 and anti-carbohydrate mAb 2D10 revealed differences in the extent of conformational flexibility in their Ag-combining sites. With regard to the enthalpy contributions for mAb 2D10 binding to 12-mer, highly favorable ΔH_a was aided by a large unfavorable ΔH_d (Fig. 3*B*). Although the trends were similar, significantly smaller changes in enthalpy were observed for mAb 7C4 binding to 12-mer especially during the association phase. This resulted in a larger favorable ΔH_{eq} for mAb 2D10 than for mAb 7C4 binding to the same Ag. However, in the case of mAb 2D10, the large favorable ΔH_{eq} is severely attenuated by unfavorable entropic changes, with the changes in $T\Delta S_a$ being highly unfavorable and $T\Delta S_d$ marginally favorable (Fig. 3*C*). In contrast, the entropy changes during both phases were relatively smaller and unfavorable during mAb 7C4-12-mer complexation. Despite binding to the 12-mer Ag by both the Abs being enthalpy driven, the high entropy penalty paid by the anti-mannopyranoside Ab suggests that major conformational changes accompany the binding of the peptide unlike relatively minor structural adjustments in the anti-12-mer Ab paratope.

Structure of the Ab paratope

The V regions of the L and H chains of the anti-peptide mAb 7C4 were sequenced to ascertain the nature of residues that form the Ag-binding site and to assign their germline origins. Five of the six CDRs could be assigned to the known classes of canonical structures: L1:9, L2:1, L3:6, H1:1, and H2:3 (20, 21). Analysis of the amino acid sequences showed that CDR H3, which is the specificity defining loop, had a larger proportion (9 of 12) of aromatic/hydrophobic residues vis-à-vis other CDRs (Fig. 4*A*). Ig-basic local alignment search tool sequence homology search (15) was conducted to assign germline origin and identify relatedness, if any, with other Abs analyzed in the context of mimicry. The germline genes were identified for the V and J elements of the L chain and the V, D, and J elements of the H chain. The L chain of mAb 7C4 belonged to the λ family to which only 5% of all mouse L chains belong (22). It had 98.3% identity with the V_L1 and 100% identity to J_L1 germline sequence. The V region of the H chain of mAb 7C4 originated from the V_HGal55.1 V gene segment while the D region bears 100% homology to DFL16.2, and the J region has 92% homology to the J_H3 segment. Interestingly, the anti-peptide Ab 7C4 shares its germline origin with Abs generated in an anti-galactan response (23) although different from the anti-mannopyranoside mAbs 2D10 and 1H7 (12). It has been previously suggested that anti-sugar Abs probably share a common origin, especially for the H chain (24). In other words, a common pool of germline gene segments may be used for immune responses against not just carbohydrates but also their peptide mimics and other nonproteinaceous haptens.

The structure of the V region of the anti-12-mer Ab 7C4 was homology modeled using the structure of a catalytic Ab, 34E4 (PDB ID: 1Y0L), as template. The H and L chains of the Ab 34E4 showed 74 and 85% sequence identity with those of mAb 7C4. Model building involved transfer of coordinates of the backbone and the identical side chains of the Fv region from 1Y0L to the sequence of 7C4 and selection of the optimum set of coordinates for the CDR H3 loop by searching the PDB database. The resultant structure was energy minimized and stereochemically validated.

Fig. 4*B* depicts the Ag-binding site of the 7C4 Ab. As observed from the sequence analysis, there are a large proportion of aromatic residues in the Ab paratope contributed by CDR H3 and L3 loops. The Ag-combining site appears to have an elongated region that is lined by these aromatic residues (Fig. 4*C*). This clustering of aromatic residues, mainly from the specificity determining CDR H3, suggests that the binding of Ags, both peptide as well as carbohydrate, may be dominated by nonpolar interactions involving aromatic residues.

Epitope mapping on the peptide Ag

Having established that the anti-peptide mAb 7C4 binds the 12-mer and mannopyranoside to a comparable extent, it was pertinent to explore the epitope on the peptide that the Ab specifically recognized. This is relevant considering that the motif, Tyr-Pro-Tyr, is thought to be a specific mimic of mannopyranoside (13, 14). Additionally, the influence of aromatic cluster in the Ab paratope on the nature of interactions involved in peptide recognition was meant to be probed. We therefore identified the residues of the

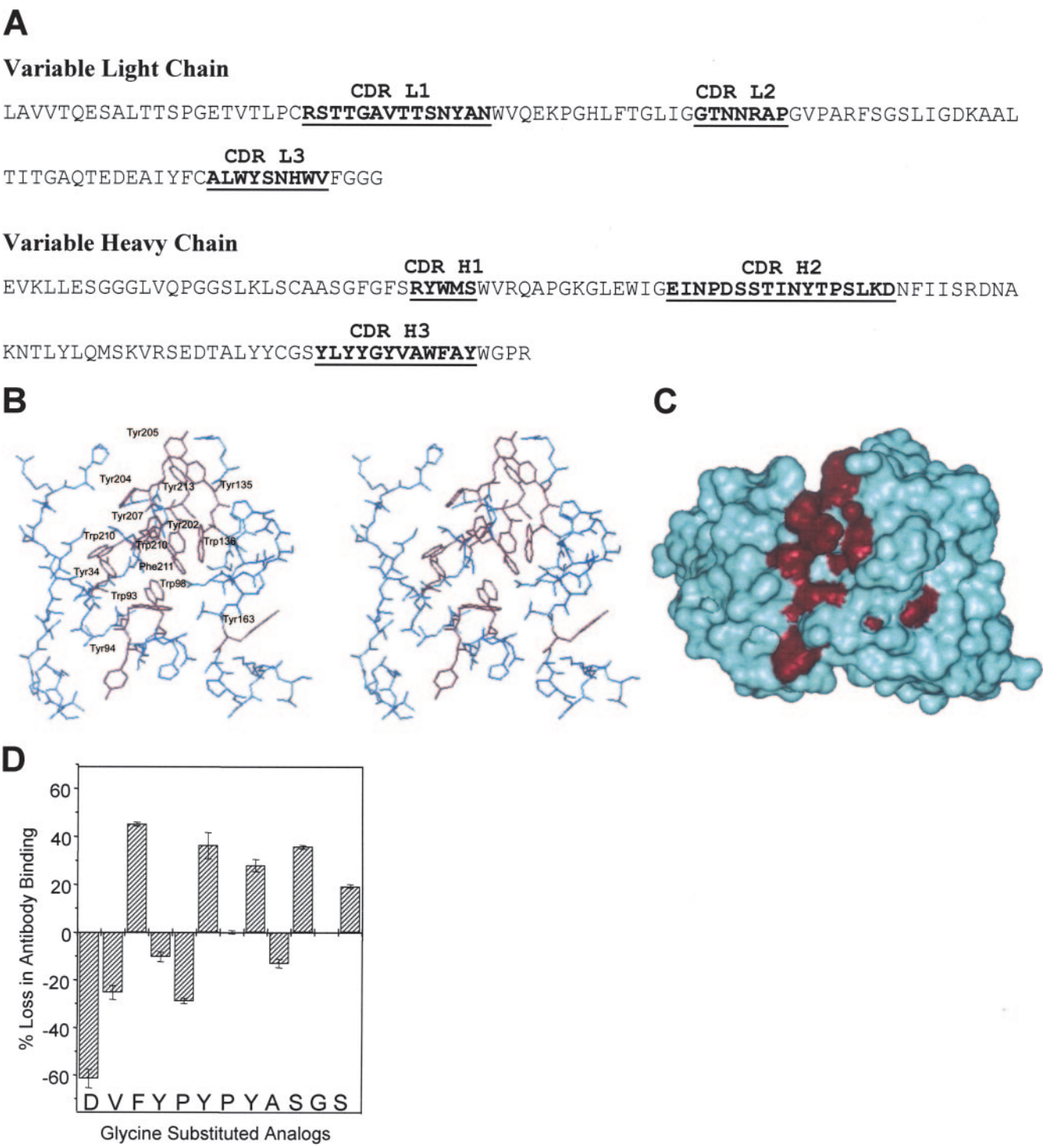

FIGURE 4. Structural features of the Ag-Ab interaction involving the mimicry-recognizing anti-peptide mAb 7C4. *A*, Amino acid sequence of the variable L and H chains of the Ab with the six CDRs highlighted. *B*, Stereo representation highlighting the presence of a large proportion of aromatic residues (colored in brown) that line the Ag-binding site. The L and the H chain residues are numbered from 1 to 103 and 104 to 217, respectively. *C*, Connolly surface of the Ab depicting the clustering of aromatic amino acids which are colored brown. *D*, Epitope mapping of 12-mer peptide for Ab 7C4 binding using glycine-substituted analogs. Higher loss in Ab binding on mutation of a particular residue would suggest that it may be critical for recognition. The bars depict the mean percentage SEM.

12-mer directly involved in recognition by the mAb 7C4 by sequentially mutating each residue to glycine and evaluating Ab binding to the peptide analog.

The three hydrophobic residues, i.e., Phe^{3}, Tyr^{6}, and Tyr^{8}, wherein Tyr^{6} and Tyr^{8} are part of the second Tyr-Pro-Tyr motif of the 12-mer, were found to be important for binding to the Ab in addition to the two serine residues, Ser^{10} and Ser^{12} (Fig. 4*D*). The average loss in binding to Phe3Gly, Tyr6Gly, or Tyr8Gly mutants was greater for mAb 7C4 as compared with other Abs that recognize the 12-mer-mannopyranoside mimicry (12), suggesting a more significant role for these hydrophobic residues in binding. The recognition pattern indicated that alternate residues are important for binding, implying that the peptide may be bound such that a face of it interacted with the Ab, while intervening side

chains may be exposed to the solvent. The role of the two serine residues in binding had been highlighted in earlier experiments involving polyclonal Abs (4). However, the epitope on the 12-mer recognized by the Ab differs from that of Con A which binds the Tyr-Pro-Tyr motif indicating that the interactions between mAb 7C4 and 12-mer may differ from those between the lectin and the peptide (5).

Discussion

The immune system is remarkable in its ability to counter a limitless array of Ags that are varied in their chemical nature and structure. What is even more extraordinary is that the vast recognition repertoire is combined with exquisite specificity of the response against any invading Ag. However, molecular mimicry which results in the functional similarity of chemically independent Ags may be a manifestation of the breakdown in this specificity of immune recognition. We had previously addressed the functional mimicry between methyl-α-D-mannopyranoside and a Tyr-Pro-Tyr motif containing dodecapeptide in the context of polyclonal immune responses (4, 7). Molecular analyses of the physiological responses against the mimicking Ags necessitated generation of mAbs and comparison of their differential recognition specificities. The mAb 7C4, raised against the 12-mer, binds to the mimicking carbohydrate moiety in addition to the peptide immunogen. The two Ags could compete with one another and bind with comparable affinity to the Ab. Furthermore, similar binding kinetics at ambient temperature suggested possibility of a common mode of recognition of the peptide and the carbohydrate Ag by the Ab 7C4.

Thermodynamic and energetic analyses of binding provided insights into the mode of interaction of mAb 7C4 with 12-mer and mannopyranoside. Binding of the Ab to both the Ags appears to be considerably independent of changes in temperature. Although the association rate constants during binding to either 12-mer or mannopyranoside remain almost unchanged with respect to temperature, marginal increase in k_d results in a minor loss in affinity of the 12-mer-Ab interaction. In terms of the temperature-dependent changes in ΔG_{eq} for binding to peptide or carbohydrate Ag, mAb 7C4 behaved differently from the mimicry-recognizing Ab 2D10 that was raised against mannopyranoside. Interestingly, the thermodynamic behavior of mAb 7C4 was similar to the mannopyranoside-specific Ab 1H7, which did not recognize carbohydrate-peptide mimicry (12).

The lack of significant temperature-dependent variation in the kinetics of binding indicates the absence of unrestricted flexibility in the Ag-combining site (17, 25). Deficiency in entropy penalty may also be indicative of the minor role of conformational alteration in the paratope during complexation with either Ag (26). In contrast, favorable entropy contribution during binding of mannopyranoside highlights the importance of hydrophobic/aromatic associations (27, 28, 19). Thus, it can be inferred that the binding of the Ab 7C4 to the two ligands does not involve large structural changes in the backbone of the CDR loops. However, minor variation in the side chain orientations is possible. Consequently, unlike the anti-mannopyranoside mAb 2D10, manifestation of mimicry in the anti-12-mer Ab 7C4 may not be attributable to conformational flexibility in the paratope that allows for the possible existence of multiple and/or additional Ag-binding subsites in dynamic equilibrium.

It was indeed intriguing that neither paratope conformational flexibility nor epitope structural similarity facilitated recognition of the chemically distinct yet mimicking 12-mer and mannopyranoside by mAb 7C4. Exploring alternative explanations for the mimicry, nature of the residues involved in the epitope-paratope interaction was analyzed. It was observed that the L chain of Ab 7C4 belongs to the λ subfamily to which only ~5% of all mouse L chains belong, which is however, common in anti-hapten Abs (29). In contrast, the H chain of mAb 7C4, which was raised against the dodecapeptide, shares its germline origin with anti-carbohydrate Abs. It is interesting to note that V_H gene segment of mAb 7C4 was discovered from an immune response against β-(1,6)-galactan (23). Sharing of common germline origin by anti-peptide and anti-carbohydrate Abs may not be incidental but linked to molecular mimicry.

The structural model of the V region of the Ab 7C4 facilitated correlation of the topological features of the Ag-combining site with the thermodynamics of epitope-paratope interaction. The Ab paratope is characterized by predominance of aromatic residues which may mediate molecular mimicry in the absence of flexibility in the Ag-combining site. Critical involvement of aromatic residues has also been observed in carbohydrate-Ab interactions especially in the context of specificity of ligand recognition (30, 31). Epitope mapping analysis of the 12-mer peptide indicated maximum contributions from Phe^3, Tyr^6, and Tyr^8 for Ab binding. Thus, the clustering of aromatic residues in the paratope as well as in the epitope reinforced the hypothesis that plasticity associated with aromatic (hydrophobic and π-π) and van der Waals interactions dominate in recognition of the 12-mer and mannopyranoside, both of which possess ring-like structural components with associated aromaticity.

It is important to note that 12-mer and mannopyranoside are functionally equivalent to an impressive extent although they do not share a high level of structural similarity (4, 7). The two Ags bind to the Ab 7C4 with high affinity and specificity mediated by interactions involving aromatic residues, especially tyrosine. Such interactions are known to broaden the specificity repertoires of not just Abs but have also been implicated in receptor-ligand, enzyme-substrate, and lectin-carbohydrate multispecificity (32–37). Significance of aromatic residues in defining the specificity of epitope-paratope interaction has been extensively addressed, highlighting the importance of tyrosine residues. It has been suggested that this residue is capable of mediating favorable interactions with a diverse array of surfaces endowing the amino acid with a privileged role in Ag recognition (38). Numerous Ab CDR H3s have been identified with high tyrosine content and many of these Abs possess diversity in their recognition potential (39).

Our laboratory has explored diverse aspects of molecular mimicry in terms of immune responses or receptor binding (4–12). The correspondence between mannopyranoside and 12-mer provided an elegant model for correlating functional and structural aspects of molecular mimicry. The functional similarity between the two mimicking ligands in the humoral immune response, both at the monoclonal as well as at the polyclonal level, was overwhelmingly more significant than the topological relationship between these Ags. Despite insufficient structural correlation, polyclonal Abs elicited against the 12-mer could recognize the carbohydrate mimic and the peptide can act as a booster for enhancing the anti-mannopyranoside immune response and vice versa (4, 7). Thus, the two Ags exhibit functional similarity in the context of the humoral immune response. Similar binding to a common receptor by ligands with limited or no apparent structural similarity has also been illustrated in case of other promiscuous Abs (40, 41).

Structural equivalence, involving not just similarity of shape and charge but also conservation of key interaction features in terms of a definable motif, such as a network of hydrogen bonds, would appear to be the most obvious rationale for functional mimicry (6, 10, 11). Contrary to expectations, molecular analyses of the anti-peptide and anti-carbohydrate Ab responses revealed diverse

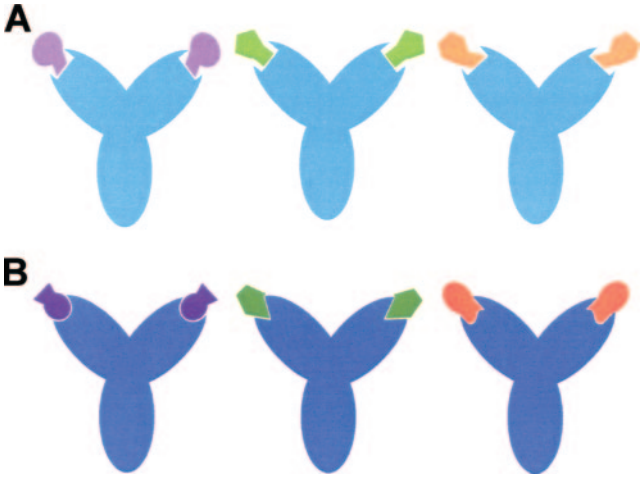

FIGURE 5. Multiple modes of molecular mimicry. Schematic representation of alternate modes of molecular mimicry in the Ab response in the absence of well-defined structural similarity between the Ags. Although the Ab is depicted in blue, the chemically diverse Ags are colored differentially. *A*, A common conformation of the Ab paratope may bind independent epitopes that are dominated by similar aromatic structures. The plasticity associated with nonpolar interactions primarily involving aromatic residues is used in binding to different mimicking Ags. *B*, Ab may adopt diverse conformations induced by independent epitopes having distinct structures facilitated by conformational flexibility of the paratope.

modes of recognition of mimicking Ags in the absence of overt structural equivalence between them (Fig. 5). By virtue of their nature, plasticity associated with aromatic/hydrophobic interactions allows the binding of mimicking Ags (Fig. 5*A*). As seen in the present analysis with anti-peptide Ab 7C4, clustering of aromatic residues in the Ab paratope allowed binding of mimicking Ags, especially those that possess ring-like structures that can stack using van der Waals and hydrophobic associations overlaid by π-π interactions. Stacking of the ring-like structures of the Ags with those from the binding site can occur in a variety of ways as the rings can slide over each other with multiple energy minima. This could potentially allow chemically dissimilar Ags like carbohydrates and peptides to behave as functional equivalents. In addition to aromatic interactions, a combination of other noncovalent interactions could also bring about such plasticity—while maintaining structural integrity—of the binding site resulting in functional mimicry.

Another mechanism for manifestation of molecular mimicry is the invocation of conformational flexibility in the paratope (Fig. 5*B*). Existence of multiple conformational states of the Ag-combining site, in dynamic equilibrium, could potentially allow for the binding of various functional mimics. The mimicry-recognizing anti-carbohydrate Ab 2D10 exemplified this mode of molecular mimicry. In contrast, the paratope of the mannopyranoside specific mAb 1H7 perhaps is predesigned for the sugar immunogen and therefore does not bind to the peptide mimic (12). Alternatively, conformational flexibility in the Ag can also augment effective mimicry (9). Additional relevant factors that could modulate molecular recognition in favor of mimicry include cementing by innocuous molecules including ions and solvent molecules resulting in improvement in shape and/or electrostatic complementarity between the paratope and epitope (10, 42).

Molecular mimicry was commonly considered to manifest by topological equivalence between the Ags with the Ab receptors possessing well-defined structures. It was also anticipated to manifest without topological equivalence between the Ags if the paratope was capable of changing structure to complement the epitopes. Our present studies have revealed molecular mimicry in the absence of either structural similarity of the epitopes or conformational flexibility in the paratope. The adaptable nature of interactions between the Ab and the Ags arising from plasticity inherent to aromatic/hydrophobic interactions illustrated a distinctive mode of binding of mimicking Ags to a common conformation of the Ab paratope. Molecular mimicry being modulated by receptor-specific properties is relevant in the context of pathogens changing their antigenic determinants for evading immune surveillance; the immune system needs to recognize altered Ags despite their structural differences. Therefore, physiological responses against the invading pathogens may include immune receptors with broader recognition specificities to minimize the consequences of antigenic variation.

Acknowledgments

We thank Drs. K. Suguna and D. K. Sethi for useful discussions and H. S. Sarna and Sushma Nagpal for technical assistance.

Disclosures

The authors have no financial conflict of interest.

References

1. Baum, H., P. Butler, H. Davies, M. J. Sternberg, and A. K. Burroughs. 1993. Autoimmune disease and molecular mimicry: A hypothesis. *Trends Biochem. Sci.* 18: 140–144.
2. Ray, S. K., C. Putterman, and B. Diamond. 1996. Pathogenic autoantibodies are routinely generated during the response to foreign antigen: a paradigm for autoimmune disease. *Proc. Natl. Acad. Sci. USA* 93: 2019–2024.
3. Monzavi-Karbassi, B., G. Cunto-Amesty, P. Luo, and T. Kieber-Emmons. 2002. Peptide mimotopes as surrogate antigens of carbohydrates in vaccine discovery. *Trends Biotechnol.* 20: 207–214.
4. Kaur, K. J., S. Khurana, and D. M. Salunke. 1997. Topological analysis of the functional mimicry between a peptide and a carbohydrate moiety. *J. Biol. Chem.* 272: 5539–5543.
5. Jain, D., K. Kaur, B. Sundaravadivel, and D. M. Salunke. 2000. Structural and functional consequences of peptide-carbohydrate mimicry: crystal structure of a carbohydrate-mimicking peptide bound to concanavalin A. *J. Biol. Chem.* 275: 16098–16102.
6. Jain, D., K. J. Kaur, M. Goel, and D. M. Salunke. 2000. Structural basis of functional mimicry between carbohydrate and peptide ligands of Con A. *Biochem. Biophys. Res. Commun.* 272: 843–849.
7. Kaur, K. J., D. Jain, M. Goel, and D. M. Salunke. 2001. Immunological implications of structural mimicry between a dodecapeptide and a carbohydrate moiety. *Vaccine* 19: 3124–3130.
8. Jain, D., K. J. Kaur, and D. M. Salunke. 2001. Plasticity in protein-peptide recognition: crystal structures of two different peptides bound to Concanavalin A. *Biophys. J.* 80: 2912–2921.
9. Jain, D., K. J. Kaur, and D. M. Salunke. 2001. Enhanced binding of a rationally designed peptide ligand of concanavalin A arises from improved geometrical complementarity. *Biochemistry* 40: 12059–12066.
10. Goel, M., D. Jain, K. J. Kaur, R. Kenoth, B. G. Maiya, M. J. Swamy, and D. M. Salunke. 2001. Functional equality in the absence of structural similarity: an added dimension to molecular mimicry. *J. Biol. Chem.* 276: 39277–39281.
11. Nair, D. T., K. J. Kaur, K. Singh, P. Mukherjee, D. Rajagopal, A. George, V. Bal, S. Rath, K. V. Rao, and D. M. Salunke. 2003. Mimicry of native peptide antigens by the corresponding retro-inverso analogs is dependent on their intrinsic structure and interaction propensities. *J. Immunol.* 170: 1362–1373.
12. Goel, M., L. Krishnan, S. Kaur, K. J. Kaur, and D. M. Salunke. 2004. Plasticity within the antigen-combining site may manifest as molecular mimicry in the humoral immune response. *J. Immunol.* 173: 7358–7367.
13. Scott, J. K., D. Loganathan, R. B. Easley, X. Gong, and I. J. Goldstein. 1992. A family of concanavalin A-binding peptides from a hexapeptide epitope library. *Proc. Natl. Acad. Sci. USA* 89: 5398–5402.
14. Oldenburg, K. R., D. Loganathan, I. J. Goldstein, P. G. Schultz, and M. A. Gallop. 1992. Peptide ligands for a sugar-binding protein isolated from a random peptide library. *Proc. Natl. Acad. Sci. USA* 89: 5393–5397.
15. Altschul, S. F., T. L. Madden, A. A. Schaffer, J. Zhang, Z. Zhang, W. Miller, and D. J. Lipman. 1997. Gapped BLAST and PSI-BLAST: a new generation of protein database search programs. *Nucleic Acids. Res.* 25: 3389–3402.
16. Laskowski, R. A., M. W. MacArthur, D. S. Moss, and J. M. Thornton. 1993. PROCHECK: a program to check the stereochemical quality of protein structures. *J. Appl. Crystallogr.* 26: 283–291.
17. Nielsen, P. K., B. C. Bonsager, C. R. Berland, B. W. Sigurskjold, and B. Svensson. 2003. Kinetics and energetics of the binding between barley α-amylase/subtilisin inhibitor and barley α-amylase 2 analyzed by surface plasmon resonance and isothermal titration calorimetry. *Biochemistry* 42: 1478–1487.

18. Wild, M. K., M. C. Huang, U. Schulze-Horsel, P. A. van der Merwe, and D. Vestweber. 2001. Affinity, kinetics, and thermodynamics of E-selectin binding to E-selectin ligand-1. *J. Biol. Chem.* 276: 31602–31612.
19. Kauzmann, W. 1959. Some factors in the interpretation of protein denaturation. *Adv. Protein Chem.* 14: 1–63.
20. Chothia, C., and A. M. Lesk. 1987. Canonical structures for the hypervariable loops of immunoglobulins. *J. Mol. Biol.* 196: 901–917.
21. Chothia, C., A. M. Lesk, A. Tramontano, M. Levitt, S. J. Smith-Gill, G. Air, S. Sheriff, E. A. Padlan, D. Davies, W. R. Tulip, et al. 1989. Conformations of immunoglobulin hypervariable regions. *Nature* 342: 877–883.
22. Almagro, J. C., I. Hernandez, M. C. Ramirez, and E. Vargas-Madrazo. 1998. Structural differences between the repertoires of mouse and human germline genes and their evolutionary implications. *Immunogenetics* 47: 355–363.
23. Hartman, A. B., and S. Rudikoff. 1984. V_H genes encoding the immune response to β-(1,6)-galactan: somatic mutation in IgM molecules. *EMBO J.* 3: 3023–3030.
24. Harris, S. L., L. Craig, J. S. Mehroke, M. Rashed, M. B. Zwick, K. Kenar, E. J. Toone, N. Greenspan, F. I. Auzanneau, J. R. Marino-Albernas, et al. 1997. Exploring the basis of peptide-carbohydrate crossreactivity: evidence for discrimination by peptides between closely related anti-carbohydrate antibodies. *Proc. Natl. Acad. Sci. USA* 94: 2454–2459.
25. Manivel, V., N. C. Sahoo, D. M. Salunke, and K. V. Rao. 2000. Maturation of an antibody response is governed by modulations in flexibility of the antigen-combining site. *Immunity* 13: 611–620.
26. De Genst, E., F. Handelberg, A. Van Meirhaeghe, S. Vynck, R. Loris, L. Wyns, and S. Muyldermans. 2004. Chemical basis for the affinity maturation of a camel single domain antibody. *J. Biol. Chem.* 279: 53593–53601.
27. Brokx, R. D., M. M. Lopez, H. J. Vogel, and G. I. Makhatadze. 2001. Energetics of target peptide binding by calmodulin reveals different modes of binding. *J. Biol. Chem.* 276: 14083–14091.
28. Ely, L. K., T. Beddoe, C. S. Clements, J. M. Matthews, A. W. Purcell, L. Kjer-Nielsen, J. McCluskey, and J. Rossjohn. 2006. Disparate thermodynamics governing T cell receptor-MHC-I interactions implicate extrinsic factors in guiding MHC restriction. *Proc. Natl. Acad. Sci. USA* 103: 6641–6646.
29. Taketani, M., A. Naitoh, N. Motoyama, and T. Azuma. 1995. Role of conserved amino acid residues in the complementarity determining regions on hapten-antibody interaction of anti-(4-hydroxy-3-nitrophenyl) acetyl antibodies. *Mol. Immunol.* 32: 983–990.
30. Vyas, N. K., M. N. Vyas, M. C. Chervenak, M. A. Johnson, B. M. Pinto, D. R. Bundle, and F. A. Quiocho. 2002. Molecular recognition of oligosaccharide epitopes by a monoclonal Fab specific for *Shigella flexneri* Y lipopolysaccharide: x-ray structures and thermodynamics. *Biochemistry* 41: 13575–13586.
31. Villeneuve, S., H. Souchon, M. M. Riottot, J. C. Mazie, P. S. Lei, C. P. J. Glaudemans, P. Kovac, J. M. Fournier, and P. M. Alzari. 2000. Crystal structure of an anti-carbohydrate antibody directed against *Vibrio cholera* O1 in complex with antigen: molecular basis for serotype specificity. *Proc. Natl. Acad. Sci. USA* 97: 8433–8438.
32. Cunningham, P., I. Afzal-Ahmed, and R. J. Naftalin. 2006. Docking studies show that D-glucose and quercetin slide through the transporter GLUT1. *J. Biol. Chem.* 281: 5797–5803.
33. Droupadi, P. R., J. M. Varga, and D. S. Linthicum. 1994. Mechanism of allergenic cross-reactions. IV. Evidence for participation of aromatic residues in the ligand binding site of two multi-specific IgE monoclonal antibodies. *Mol. Immunol.* 31: 537–548.
34. Nagpal, S., K. J. Kaur, D. Jain, and D. M. Salunke. 2002. Plasticity in structure and interactions is critical for the action of indolicidin, an antibacterial peptide of innate immune origin. *Protein Sci.* 11: 2158–2167.
35. Weis, W. I., and K. Drickamer. 1996. Structural basis of lectin-carbohydrate recognition. *Annu. Rev. Biochem.* 65: 441–473.
36. Muraki, M. 2002. The importance of CH/π interactions to the function of carbohydrate binding proteins. *Protein Pept. Lett.* 9: 195–209.
37. Borst, P., and R. O. Elferink. 2002. Mammalian ABC transporters in health and disease. *Annu. Rev. Biochem.* 71: 537–592.
38. Fellouse, F. A., P. A. Barthelemy, R. F. Kelley, and S. S. Sidhu. 2006. Tyrosine plays a dominant functional role in the paratope of a synthetic antibody derived from a four amino acid code. *J. Mol. Biol.* 357: 100–114.
39. Ramsland, P. A., C. R. Brock, J. Moses, B. G. Robinson, A. B. Edmundson, and R. L. Raison. 1999. Structural aspects of human IgM antibodies expressed in chronic B lymphocytic leukemia. *Immunotechnology* 3–4: 217–229.
40. Kramer, A., T. Keitel, K. Winkler, W. Stocklein, W. Hohne, and J. Schneider-Mergener. 1997. Molecular basis for the binding promiscuity of an anti-p24 (HIV-1) monoclonal antibody. *Cell* 91: 799–809.
41. Keitel, T., A. Kramer, H. Wessner, C. Scholz, J. Schneider-Mergener, and W. Hohne. 1997. Crystallographic analysis of anti-p24 (HIV-1) monoclonal antibody cross-reactivity and polyspecificity. *Cell* 91: 811–820.
42. Ravishankar, R., M. Ravindran, K. Suguna, A. Surolia, and M. Vijayan. 1997. Crystal structure of the peanut lectin-T-antigen complex: carbohydrate specificity generated by water bridges. *Curr. Sci.* 72: 855–861.